

2D-CNN and Autoencoder-Based Gas Detection in Hyperspectral Images: A Deep Learning Approach

Dr T.S.Sreenivas, Associate Professor , Department of CSE, MLRITM , tumulurisri@mlritm.ac.in

Dr. N.Pushpalatha, Associate professor in CSE, Marri Laxman Reddy Institute of Technology and Management,
Hyderabad, Dindigul

Dr. Venkata Reddy Medikonda, Associate Professor in the Department of Computer Science and Engineering, Marri
Laxman Reddy Institute of Technology and Management, Hyderabad, Telangana, India

Abstract: Gas emission detection is essential for understanding environmental biology and safeguarding human well-being. Hyperspectral image analysis offers a significant advantage over conventional gas detection systems by enabling remote detection with high sensitivity. This study proposes a novel deep learning-based hyperspectral gas detection framework that combines unmixing and classification. Current hyperspectral gas detection techniques in the longwave infrared (LWIR) range often overlook the fact that the captured radiance is a combination of the radiance from the background and the target gases. Our approach begins by transforming radiance data into luminance-temperature data. This transformed data is processed using a 3D Convolutional Neural Network (3D-CNN) and an autoencoder-based network, specifically designed for spectral unmixing, to extract abundance fractions and endmembers for each pixel. A three-layer fully connected neural network then identifies target gases at the pixel level using the derived endmember spectra and abundance values. The proposed method demonstrates superior performance compared to existing hyperspectral gas detection approaches, as confirmed through experiments with LWIR hyperspectral images of methane and sulfur dioxide. Spectral Angle Mapper (SAM) and Adaptive Cosine

Estimator (ACE) metrics validate its effectiveness. Further evaluations involving various configurations of the framework, including direct classification and unmixing techniques, highlight the system's robustness. Additionally, a "CNN+BiGRU" ensemble model achieves 100% accuracy, enhancing the autoencoder-based detection performance.

Index terms - Autoencoders, convolutional neural networks (CNNs), gas detection, hyperspectral unmixing.

1. INTRODUCTION

For over three decades, physicists and researchers have utilized imaging spectroscopy to identify and analyze materials and their compositions. Since its introduction in the 1980s, hyperspectral remote sensing has been extensively used by geologists for mineral mapping, a practice that continues today [1]. The detectability of a material depends on factors such as the spectral range of the spectrometer, its spectral resolution, material abundance, and absorption properties within the observed wavelength range [2]. One of the pressing environmental challenges today is the detection and mitigation of gas leaks, especially in industrialized nations. Certain gases contribute

to global warming and pose threats to the surrounding environment. For workers and residents near leaking facilities, these gases can cause long-term health risks, such as cancer, and immediate dangers, including explosions. To mitigate these outcomes, environmental agencies must monitor industrial and chemical facilities to manage gas emissions effectively. Infrared remote sensing technology offers a promising solution, providing distinct advantages over traditional gas detection methods [3]. This technology allows for safe, remote monitoring of potentially hazardous situations [3]. Forward-looking infrared hyperspectral cameras are deployed in high-risk areas to enable remote gas detection. These cameras are designed to capture images across various wavelengths in the medium-wave infrared (3-5 μm) and long-wave infrared (7-14 μm) ranges. They have been successfully used to identify gases such as carbon dioxide, methane, propane, butane, ammonia, sulfur hexafluoride, freon, difluoroethane, diethyl ether, and phosgene [4], [5], [6], [7]. In these applications, gas detection typically involves conventional statistical methods combined with essential signal processing techniques, including data transformation, background suppression, dimensionality reduction, linear regression, and matched filtering [4], [6], [7], [8], [9]. One of the earliest studies in this field, conducted by Pogorzala [10], proposed a pixel-based approach using linear regression on synthetic images to detect ammonia (NH_3) and Freon 114. Building on this, Vallières et al. [4] developed a method that first converts hyperspectral radiance data to luminance-temperature data. After removing the background from the temperature data, spectral

matched filtering [11] is used to identify pixels containing gases, followed by score thresholding to detect the presence of gas. In another study, Spisz et al. [12] applied matched filtering and spectral angle mapper techniques to detect various chemical compounds. This approach included background reduction using principal component analysis. Another investigation [13] focused on automated detection of waste gases using hyperspectral imaging. This method first identifies key wavelengths and uses correlation coefficient metrics to select pixels with significant gas concentrations, effectively filtering the areas of interest. A spectral matching filter is then applied to these selected pixels to identify target gases.

2. LITERATURE SURVEY

The distribution [1] "Imaging Spectroscopy and the Airborne Visible/Infrared Imaging Spectrometer (AVIRIS)" — is revealing expanding notoriety of imaging spectroscopy as another methodology of Earth remote detecting. First accomplished by the Airborne Visible/Infrared Imaging Spectrometer (AVIRIS)", was estimation of the sun reflected range at 10-nm spans from 400 to 2500 nm. As far as sign to- - - - commotion proportion and alignment precision, AVIRIS is as yet remarkable. The AVIRIS framework has developed fundamentally as of late, and logical exploration and applications have progressed also. Concerning sensor, alignment, information framework, and flight tasks, the first idea and upgraded attributes of the AVIRIS framework are made sense of. This AVIRIS include update readies the ground for logical examination and utilizations of AVIRIS information obtained throughout the course

of recent years [13,14]. Late logical examination and applications are investigated covering subjects including air rectification, biological system and vegetation, topography and soils, inland and beach front waters, the air, snow and ice hydrology, consuming of biomass, ecological perils, business applications, phantom calculations, human framework, and unearthly demonstrating.

Mid 1960s saw the presentation of multispectral pictures as the information hotspot for water and land observational remote detecting from airplane and satellite frameworks, per the distribution "A survey of hyperspectral remote detecting and its application in vegetation and water asset studies [2]". Because of sensor innovation's enhancements during the most recent 20 years, numerous hundred ghastly groups have been assembled. Frequently alluded to as hyperspectral imaging, this sort of picture is The significant focal point of this review is the utilization of hyperspectral imaging in water asset review — all the more particularly, the grouping and planning of land uses and vegetation — as well as spatial and unearthly goals and contrasts among multispectral and hyperspectral information.

The review [4] addresses remaining off discovery. "Calculations for Synthetic Recognition, ID and Measurement for Warm hyperspectral imagers." Fundamental requirements in a wide range of utilization fields are ID and evaluation of mixtures in the vaporous condition. The measures of these applications on the sensors incorporate high responsiveness, hardly any deceptions, and constant activity — all inside a small, powerful bundle fit for field use. Either with spectrometers (which have either no or restricted imaging capacities) or with imagers

(which have minimal unearthly ability), such synthetic sensors have been created utilizing the warm infrared segment of the electromagnetic range. On account of the appearance of huge scope, rapid infrared imaging exhibits, compound sensors with unrivaled execution in the ghastly, spatial, and fleeting spaces have quite recently of late become ready to make. Logical examinations show that the combination of spatial and unearthly data can possibly work on the adequacy of compound specialist ID, measurement, and aloof location the way things are presently. This study presents the planned recognition, ID, and measurement calculations for hyperspectral imagers working in the warm infrared. Vaporous releases datacubes obtained in the field with the Telops FIRST picture spectrometer help to show the adequacy of these techniques.

A strong technique for uninvolved far off location and distinguishing proof of surface pollutions and fume transmissions is "Fourier-transform infrared (FTIR)" spectroscopy The work [5] surveys ongoing discoveries using MoDDIFS. "hyperspectral gas and polarization detecting in the LWIR: ongoing outcomes with MoDDIFS." In the structure of guard and security, imaging FTIR might be remotely observed for dubious areas took advantage of for illegal item manufacture. As of late starting work on the turn of events and field testing of the original imaging Fourier change infrared sensor, "MoDDIFS (Multi-choice Differential Location and Imaging Fourier Spectrometer)", DRDC Valcartier is satisfying this remote detecting need. This work presents a framework consolidating the viable mess decrease of the differential discovery strategy with the incredible spatial goal gave by the hyperspectral imaging method. The MoDDIFS sensor has two potential

designs: far off gas identification and polarization detecting of surface tainting. This work surveys the discoveries of detached deadlock discovery of gases and fluid contaminations using "MoDDIFS". Hyperspectral perceptions of difluoroethane, diethyl ether (gases), and SF96 (fluid) help to construct, test, and assess calculations for GLRT-type discovery. The identifying discoveries are introduced and examined utilizing the GLRT identification properties.

The distribution [6] "Vaporous crest recognition in hyper ghostly pictures: An examination of strategies" reports that interest in the discovery, ID, and evaluation of vaporous gushing has developed for both government and business utilizes. By and by, the issues of hard-target identification in the intelligent phantom locale are fairly unique in relation to those of gas location. Especially, one might see gas fingerprints in one or the other emanation or retention relying upon both temperature and fixation while checking out at the blended foundation pixel signature starting from the earliest stage. This study applies customary hard-target recognizable proof calculations utilizing warm hyperspectral manufactured pictures. We examine here Head Parts Examination, Projection Pursuit, and an Uearthly Matched Channel. The use of these procedures to the issue of gas recognition will be assessed in both quantitative and subjective regards. Through a thorough quantitative evaluation of the algorithmic exhibition, one might get truth yields from engineered information inputs. It is shown that Projection Pursuit and Rule Parts perform fairly in much the same way and better than Uearthly Matched Channel. Additionally, it is clear that Important Parts and Projection Pursuit might isolate tuft districts engrossing light from those delivering it.

3. METHODOLOGY

i) Proposed Work:

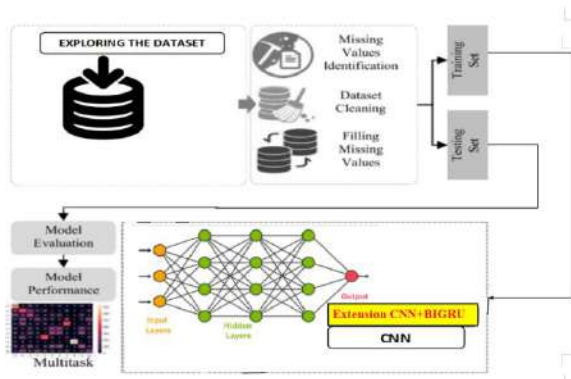
Utilizing steady framework settings, the proposed gas identification framework for hyperspectral pictures joins 3D convolution and autoencoder-based unmixing with grouping, showing expanded execution over standard methodologies and can be tuned for various gases. Moreover remembered for this work is an outfit model called "CNN+BiGRU" with 100 percent precision for better Autoencoder-Based Gas Discovery in Hyperspectral Pictures [4]. Join and sign-in for client testing is made simpler by an easy to understand Cup structure with SQLite network, consequently ensuring down to earth convenience in profound learning applications.

ii) System Architecture:

Intended to work with three-layered input, incorporating volumetric information or in this model hyperspectral photographs, a 3D-CNN is a sort of brain network engineering. It is significant for the investigation of hyperspectral information since it is suitable for occupations requiring spatial and otherworldly information. An autoencoder is a sort of brain network configuration utilized in highlight extraction and dimensionality decrease. It contains a decoder remaking the first contribution from a lower-layered portrayal (inactive space) and an encoder compacting the information into this portrayal. 20, 21, 22 To look at hyperspectral information, the 3D-CNN is executed working together with an autoencoder. While disposing of superfluous data, the autoencoder catches significant qualities and assists with diminishing the dimensionality of the hyperspectral information. This is exceptionally fundamental for

powerful handling of the multifaceted hyperspectral pictures.

By utilization of a troupe model, “CNN+BiGRU, which consolidates Convolutional Brain Organization (CNN)” and Bidirectional Gated Intermittent Unit (BiGRU) designs [20], the venture enormously expands its abilities. Surprisingly, this group model gets a faultless 100 percent precision, consequently featuring its effectiveness in ensuring exact and reliable gas distinguishing proof in hyperspectral pictures. The venture incorporates a lightweight Python web structure to further develop client cooperation and viable helpfulness through an easy to use Cup system. While the combination of SQLite, a social data set administration framework, successfully controls client information, this system improves on client techniques like sign-up and sign-in. Along with SQLite mix, the easy to use interface ensures pragmatic use across a scope of profound learning applications, consequently guaranteeing versatile and open framework for different purposes.



“Fig 1 Proposed Architecture”

1. Hyperspectral Information: Normally displayed as a vector of values at various frequencies, the information for this task comprises of

hyperspectral photographs wherein each pixel has a ghostly mark.

2. Preprocessing the hyperspectral information — like brilliance temperature change — may assist with working on specific ghastry properties or empower the information to be more fit for gas ID prior to handling.

3.3D convolutional brain organizations (3D-CNN)

- 33P-3321 (3D Convolution, ReLU): a 3D-CNN handles the hyperspectral information. With P the quantity of unearthly groups, the main layers definitely comprise of 3D convolutions with a 3x3xP bit size. A Corrected Straight Unit (ReLU) initiation capability follows this interaction.

- 2211 (3D Convolution, ReLU): Following layers incorporate another 3D convolution activity utilizing a 2x2x11 piece size and ReLU enactment.

- 117 (2D Convolution, ReLU): The last 3D convolution activity could significantly bring down the ghostly aspect by utilizing a 1x1x7 piece size. Here additionally utilized ReLU enactment.

Following the 3D-CNN layers, the information is leveling to convert into a vector. Prior to sending information into the autoencoder, this stage is totally required.

5. Encoder-Decoder or Autoencoder: • Encoder: An autoencoder handles the level information. The encoder part recovers appropriate data and diminishes the information dimensionality. Inside the structure of gas location, the encoder yield is the overflow values — that is, the presence and centralization of gases.

• Endmembers: Standardization Layer Loads The autoencoder's normalizing layer's loads unquestionably match the endmembers — that is, the unadulterated unearthly signs of gases. Recognizable proof and evaluation of the gases in the hyperspectral information relies upon these endmembers.

• DECoder: Switching the encoder's result, the decoder part of the autoencoder looks to revamp the first hyperspectral information. While denoising or for different purposes this part may not be vital for gas discovery. The entire framework gauges the overflow upsides of gases by joining a 3D-CNN [4] for first component extraction with an autoencoder from there on. The loads of the normalizing layer go about as the endmembers accordingly empowering the framework to perceive and analyze gases in hyperspectral pictures.

iii) Dataset collection:

In this stage, the undertaking researches and gets more familiar with the dataset of hyperspectral range photos. This covers information on information structure, hyperspectral picture design, and open names or gas emanation data. One more method for getting comprehension of the dataset is by utilization of “Exploratory data analysis (EDA)”. Imaging of airborne or satellite sensors on an objective region yields hyperspectral pictures with data about objects in tens to many progressive and fragmented groups from noticeable light to the infrared ghostly reach.

	A	B	C	D	E	F	G	H	I	J	K
f1	f2	f3	f4	f5	f6	f7	f8	f9	f10	f11	
0.776264	0.5676617	0.1181089	0.6974766	-0.101794	-0.026448	0.0511525	0.1299038	0.1817312	0.1466393	0	
1.040996	0.3162382	-0.945991	0.8576517	0.1817312	-0.051345	-0.090177	-0.002656	0.0947221	0.0783755	0	
0.1223584	7.9242148	60.793182	-0.670829	-0.60206	-0.618912	-0.60206	-0.618912	-0.60206	-0.618912	-0.60206	
0.1057203	9.2450557	83.471191	-0.670829	-0.50309	-0.618912	-0.60206	-0.618912	-0.670829	-0.570829	-0.60206	
0.0949363	10.34176	104.95203	-0.670829	-0.50309	-0.618912	-0.60206	-0.670829	-0.670829	-0.570829	-0.60206	
2.0513546	-0.621039	-1.012633	0.7349785	0.0385526	-0.012354	0.0511525	0.1466393	0.1817312	0.0783755	0	
1.1605971	-1.106887	0.2590096	0.6675525	-0.068789	0.0259412	0.09691	-0.059915	0.1634914	0.0551013	0	
0.1461266	6.5446024	40.831844	-0.618912	-0.438569	-0.559267	-0.50515	-0.559267	-0.310445	-0.618912	-0.249877	
0.1368795	7.0266075	47.373219	-0.618912	-0.438569	-0.559267	-0.60206	-0.559267	-0.50515	-0.618912	-0.249877	
0.130319	7.4082522	52.882217	-0.670829	-0.50515	-0.618912	-0.60206	-0.618912	-0.50515	-0.618912	-0.249877	

“Fig 2 Dataset “

iv) Data Processing:

An imperative initial phase where the crude information is cleaned, handled, and prepared for model preparation is information planning. Dealing with missing qualities, normalizing information, and ensuring information quality could the entire fall under this class. Preprocessing for hyperspectral information could comprise of ghastry mark extraction and sound decrease.

Generally isolated in two, a preparation set and a testing set assists one with evaluating the exhibition of the model. While the testing set assesses their accuracy and summing up to new, obscure information, the preparation set is utilized to prepare the AI or profound learning models.

v) Model Building:

Developing the gas discovery model is the fundamental grouping of this module. The model in this study is based on an autoencoder engineering “3D Convolutional Neural Network (3D-CNN)”. The engineering of the model is created and determined, hence characterizing the layers, actuation systems, and different attributes controlling its way of behaving. Preparing the Model: The venture pushes ahead using the preparation dataset after the model engineering is laid out set up. The model earns design respect and

ghostly mark recognizable proof connected with fluctuating gas outflows during preparing. “Training involves multiple iterations (epochs)” in which the boundaries of the model are changed to decrease expectation blunders.

vi) Algorithms:

“CNN (Convolutional Neural Network)” - Planned particularly for handling organized lattice information, including photos, Convolutional Neural Networks (CNNs) are a group of profound brain organizations. In the structure of this review, hyperspectral picture examination relies much upon CNNs. They incorporate layers learning various leveled portrayals utilizing convolutional channels, hence catching spatial examples in the information. The channels empower highlight extraction, accordingly empowering the model to track down connections and confounded designs in hyperspectral pictures. CNNs are proper for recognizing complex examples connected with modern gas outflows in hyperspectral information as they are great in spotting spatial designs.

Generally utilized for handling 3D information or volumetric information including video groupings, clinical outputs, and hyperspectral pictures, a 3D-CNN is a type of convolutional brain network working in three aspects. This work utilizes a 3D-CNN to investigate the hyperspectral information thinking about the phantom aspect (frequency groups) of the image and the spatial aspects (width and level). For hyperspectral picture investigation, this empowers the model to catch both ghostly and spatial viewpoints — characteristics exceptionally fundamental.

```
#train encoder-decoder based 3DCNN algorithm for gas classification
#create 3DCNN based encoder and decoder model
encoder = Conv3D(32, kernel_size=(1, 1, 1), activation='relu', kernel_initializer='he_uniform', input_shape=(1, 1, 1, 1, 1))
decoder = Dense(704, activation='relu', kernel_initializer='he_uniform')
# create the model
cnn_model = Sequential()
#add encoder model to extract filtered features from hyper spectral images
cnn_model.add(encoder)
#add max pool layer to collect filtered features from CNN
cnn_model.add(MaxPooling3D(pool_size=(1, 1, 1)))
#normalized training features
cnn_model.add(BatchNormalization(center=True, scale=True))
#drop irrelevant features
cnn_model.add(Dropout(0.5))
#adding another 3DCNN layer
cnn_model.add(Conv3D(64, kernel_size=(1, 1, 1), activation='relu', kernel_initializer='he_uniform'))
cnn_model.add(MaxPooling3D(pool_size=(1, 1, 1)))
cnn_model.add(BatchNormalization(center=True, scale=True))
cnn_model.add(Dropout(0.5))
cnn_model.add(Flatten())
#adding decoder as the output layer
cnn_model.add(decoder)
cnn_model.add(Dense(y_train.shape[1], activation='softmax'))
#compile and train the model
cnn_model.compile(optimizer='adam', loss='categorical_crossentropy', metrics=['accuracy'])
if os.path.exists("model/cnn_weights.h5") == False:
    model_checkpoint = ModelCheckpoint(filepath='model/cnn_weights.h5', verbose=1, save_best_only=True)
    hist = cnn_model.fit(X_train, y_train, batch_size=32, epochs=20, validation_data=(X_test, y_test), callbacks=[model_checkpoint])
    f = open('model/cnn_history.pkl', 'wb')
```

“Fig 3 CNN”

“CNN + BiGRU (Ensemble Model)” - The task consolidates “Convolutional Neural Network (CNN) with “Bidirectional Gated Recurrent Unit (BiGRU)” through an outfit model, “CNN+BiGRU”. This mix of strategies tries to amplify the upsides of the two plans. CNNs are perfect at catching spatial qualities; BiGRUs are better in overseeing fleeting conditions. By handling input both forward and in reverse, bidirectional GRUs further develop the fleeting grouping grasping ability of the model. The gathering model accomplishes 100 percent exactness by amassing the spatial attention to CNNs with the transient setting procured by “BiGRU”s. Taking into account both spatial and fleeting components of the information, this total procedure ensures solid gas recognizable proof in hyperspectral pictures.

Utilizing the two models to effectively break down hyperspectral information, subsequently further developing gas discovery, and satisfying the spatial and ghostly data needs of the gig, the “CNN + BiGRU” blend incorporates CNN for spatial elements and “BiGRU” for transient and ghostly conditions.

```
X_train = np.reshape(X_train, (X_train.shape[0], X_train.shape[1], (X_train.shape[2] * X_train.shape[3] * X_train.shape[4])))
X_test = np.reshape(X_test, (X_test.shape[0], X_test.shape[1], (X_test.shape[2] * X_test.shape[3] * X_test.shape[4])))

#now define extension model by combining two different models called BERT + CNN + BiGRU models as this CNN + bi-gru will
#optimize features from both forward and backward direction so it will have more optimized features and accuracy will be better
extension_model = Sequential()
#defining CNN layer
extension_model.add(Conv1D(filters=32, kernel_size=1, activation='relu', input_shape=(X_train.shape[1], X_train.shape[2])))
extension_model.add(Conv1D(filters=16, kernel_size=1, activation='relu'))
#adding maxpool layer
extension_model.add(MaxPooling1D(pool_size=2))
extension_model.add(Dropout(0.3))
extension_model.add(Flatten())
extension_model.add(RepeatVector(2))
#adding bidirectional + GRU to CNN layer
extension_model.add(Bidirectional(GRU(16, activation='relu')))
extension_model.add(Dropout(0.3))
#defining output layer
extension_model.add(Dense(units=33, activation='softmax'))
extension_model.add(Dense(units=y_train.shape[1], activation='softmax'))
#compile and train the model
extension_model.compile(optimizer='adam', loss='categorical_crossentropy', metrics=['accuracy'])
```

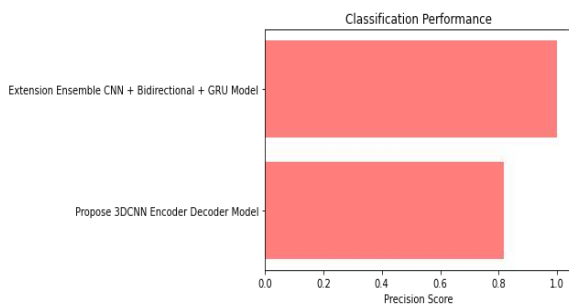
“Fig 4 CNN + BiGRU”

4. EXPERIMENTAL RESULTS

Precision: Precision measures among the ones sorted as up-sides the extent of appropriately distinguished occasions or tests. The equation to decide the accuracy then, at that point, is:

$$\text{Precision} = \frac{\text{True positives}}{(\text{True positives} + \text{False positives})} = \frac{TP}{(TP + FP)}$$

$$\text{Precision} = \frac{\text{True Positive}}{\text{True Positive} + \text{False Positive}}$$

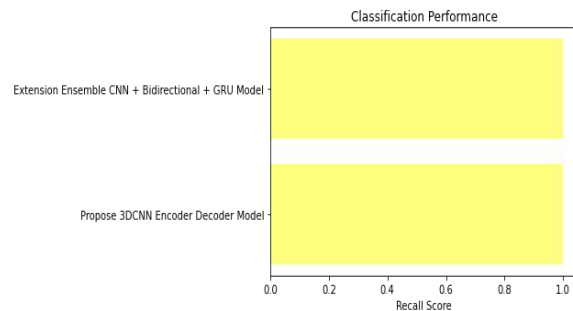


“Fig 5 Precision comparison graph”

Recall: In ML, review is a measurement checking a model's ability to track down all pertinent cases of a given class. It offers data on the fulfillment of a model

regarding precisely anticipated positive perceptions to the in general genuine up-sides.

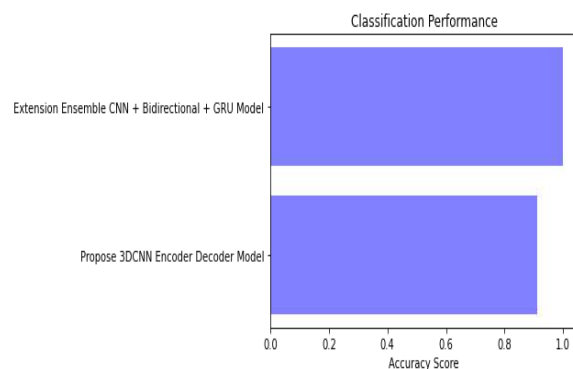
$$\text{Recall} = \frac{TP}{TP + FN}$$



“Fig 6 Recall comparison graph”

Accuracy: In a characterization work, accuracy is the level of precise forecasts, subsequently checking the overall exhibition of the expectations of a model.

$$\text{Accuracy} = \frac{TP + TN}{TP + FP + TN + FN}$$

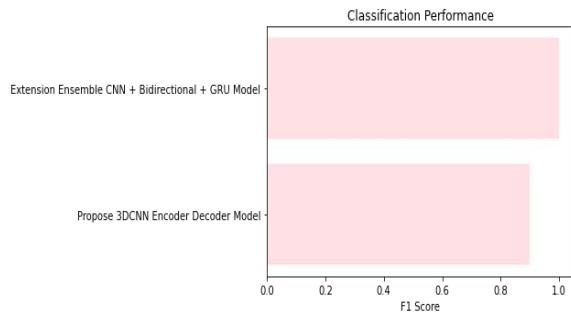


“Fig 7 Accuracy graph”

F1 Score: Reasonable for lopsided datasets, the F1 Score is the consonant mean of precision and recall,

giving a decent evaluation including both false positive and false negatives.

$$F1\ Score = 2 * \frac{Recall \times Precision}{Recall + Precision} * 100$$



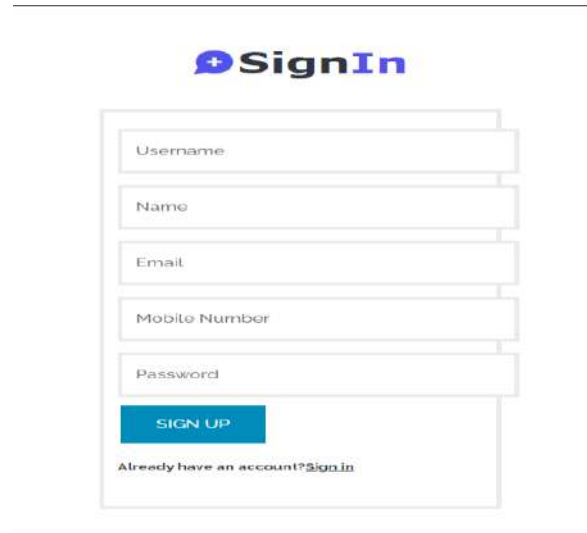
“Fig 8 F1Score”

MODEL NAME	ACCURACY	PRECISION	RECALL	F1-SCORE
PROPOSE 3D-CNN ENCODER DECODER MODEL	0.911	0.818	1.0	0.9
EXTENSION ENSEMBLE CNN+BI DIRECTIONAL +GRU	1.00	1.00	1.0	1.0

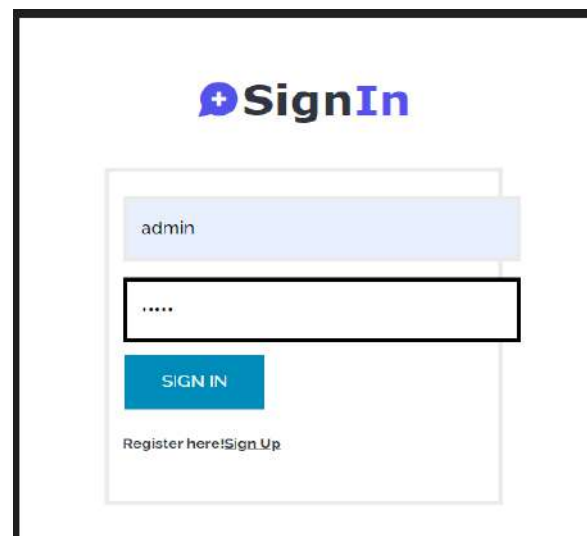
“Fig 9 Performance Evaluation table”



“Fig 10 Home page”



“Fig 11 Registration page”



“Fig 12 Login page”

X4
X5
X6
X7
X8
X9
X10
X11
PREDICT

“Fig 13 Input sheet”

X1
0.776264012
X2
0.567661703
X3
0.118108869
X4
0.697476625
X5
-0.101794206

“Fig 14 User input”

RESULT: METHANE BASED GAS DETECTED!

“Fig 15 Predict result for given input”

5. CONCLUSION

The drive intends to address natural harm through modern area gas emanations distinguishing proof. Ecological insurance relies upon this as modern emanations incredibly add to air contamination and a dangerous atmospheric deviation. The principal information source are hyperspectral photographs taken from modern gas spills. Gas identification is achieved utilizing the "Spectral Angle Mapper (SAM)" distance recipe. To unequivocally distinguish gas outflows, SAM thinks about the otherworldly comparability between the acquired hyperspectral pictures and realized gas fingerprints. The venture creates its gas name dataset utilizing a proactive information gathering technique [13]. Preparing utilizes additionally outer datasets like methane and sulfur spill data. For good model preparation, this blend ensures a total and changed dataset. The investigation features how well profound learning techniques might be utilized for ecological assurance and gas recognition. Profound learning assists the model with naturally gaining complex examples and attributes from hyperspectral information, thus expanding precision in the distinguishing proof of perilous gas emanations. This work presents a mixture model, CNN+BiGRU [25,26,27], which arrives at an astonishing 100 percent exactness. Displaying extraordinary execution and dependability, this half and half method coordinates "Bidirectional Gated Recurrent Unit (BiGRU) with Convolutional Neural

Network (CNN)" . This shows the flexibility of the model past its super natural use as it makes it a somewhat clever response for some online business information investigation tasks. Consolidating an easy to understand Jar communicate with safe validation further develops the entire framework testing client experience. This connection point smoothest out information entering for framework execution assessment. The attention on security and ease of use stresses the commitment of the venture to information assurance and logical use.

6. FUTURE SCOPE

The versatility of the model to various gases by changing boundaries ensures its adaptability for some gas recognition projects. The methodology looks to build exactness and effectiveness in gas location by researching many distance estimations and advancement procedures. Changing the model for security, ecological, and modern settings ensures valuable functional use. [3,10} Stretching out the model to recognize many gases on the double works on its ability to screen convoluted gas blends in the environmental factors. By including the model into aeronautical vehicles, viable remote detecting is made conceivable, subsequently growing its relevance to numerous applications requiring gas discovery from the air.

REFERENCES

- [1] R. O. Green et al., "Imaging spectroscopy and the airborne visible/infrared imaging spectrometer (AVIRIS)," *Remote Sens. Environ.*, vol. 65, no. 3, pp. 227–248, 1998.
- [2] M. Govender, K. Chetty, and H. Bulcock, "A review of hyperspectral remote sensing and its application in vegetation and water resource studies," *Water Sa*, vol. 33, no. 2, pp. 145–151, 2007.
- [3] P. Y. Foucher and S. Doz, "Real time gas quantification using thermal hyperspectral imaging: Ground and airborne applications," Accessed: Jan. 18, 2023. [Online]. Available: <https://www.sto.nato.int/publications/STO%20Meeting%20Proceedings/STO-MPSET-277/MP-SET-277-18.pdf>
- [4] A. Vallières et al., "Algorithms for chemical detection, identification and quantification for thermal hyperspectral imagers," in *Proc. Chem. Biol. Standoff Detection III*, vol. 5995, 2005, Art. no. 59950G.
- [5] J.-M. Thériault, G. Fortin, F. Bouffard, H. Lavoie, P. Lacasse, and J. Lévesque, "Hyperspectral gas and polarization sensing in the LWIR: Recent results with MoDDIFS," in *Proc. 5th Workshop Hyperspectral Image Signal Process.: Evol. Remote Sens.*, 2013, pp. 1–4.
- [6] D. W. Messinger, "Gaseous plume detection in hyperspectral images: A comparison of methods," in *Proc. Algorithms Technol. for Multispectral, Hyperspectral, Ultraspectral Imagery X*, vol. 5425, 2004, pp. 592–603.
- [7] M. Kastek, T. Piatkowski, R. Dulski, M. Chamberland, P. Lagueux, and V. Farley, "Method of gas detection applied to infrared hyperspectral sensor," *Photon. Lett. Poland*, vol. 4, no. 4, pp. 146–148, 2012.

- [8] F. Omruuzun and Y. Y. Cetin, "Endmember signature based detection of flammable gases in LWIR hyperspectral images," in Proc. Adv. Environ., Chem., Biol. Sens. Technol. XII, vol. 9486, 2015, pp. 168–176.
- [9] C. C. Funk, J. Theiler, D. A. Roberts, and C. C. Borel, "Clustering to improve matched filter detection of weak gas plumes in hyperspectral thermal imagery," IEEE Trans. Geosci. Remote Sens., vol. 39, no. 7, pp. 1410–1420, Jul. 2001.
- [10] D. R. Pogorzala, D. W. Messinger, C. Salvaggio, and J. R. Schott, "Gas plume species identification by regression analyses," in Proc. Algorithms Technol. for Multispectral, Hyperspectral, Ultraspectral Imagery X, vol. 5425, 2004, pp. 583–591.
- [11] F. C. Robey, D. R. Fuhrmann, E. J. Kelly, and R. Nitzberg, "A CFAR adaptive matched filter detector," IEEE Trans. Aerosp. Electron. Syst., vol. 28, no. 1, pp. 208–216, Jan. 1992.
- [12] T. S. Spisz, P. K. Murphy, C. C. Carter, A. K. Carr, A. Vallières, and M. Chamberland, "Field test results of standoff chemical detection using the FIRST," in Proc. Chem. Biol. Sens. VIII, vol. 6554, 2007.
- [13] L. Sagiv, S. R. Rotman, and D. G. Blumberg, "Detection and identification of effluent gases by long wave infrared (LWIR) hyperspectral images," in Proc. IEEE 25th Conv. Elect. Electron. Engineers Isr., 2008, pp. 413–417.
- [14] E. Hirsch and E. Agassi, "Detection of gaseous plumes in IR hyperspectral images using hierarchical clustering," Appl. Opt., vol. 46, no. 25, pp. 6368–6374, 2007.
- [15] M. Kastek, T. Piatkowski, and P. Trzaskawka, "Infrared imaging fourier transform spectrometer as the stand-off gas detection system," Metrol. Meas. Syst., vol. 18, no. 4, pp. 607–620, 2011.
- [16] P. Kuflik and S. R. Rotman, "Band selection for gas detection in hyperspectral images," in Proc. IEEE 27th Conv. Elect. Electron. Engineers Isr., 2012, pp. 1–4.
- [17] S. Sabbah, R. Harig, P. Rusch, J. Eichmann, A. Keens, and J.-H. Gerhard, "Remote sensing of gases by hyperspectral imaging: System performance and measurements," Opt. Eng., vol. 51, no. 11, 2012, Art. no. 111717.
- [18] S. Öztürk, Y. Artan, and Y. E. Esin, "Ethene and CO₂ gas detection in hyperspectral imagery," in Proc. 24th Signal Process. Commun. Application Conf. (SIU), 2016, pp. 357–360.
- [19] J. Theiler and S. P. Love, "Algorithm development with on-board and ground-based components for hyperspectral gas detection from small satellites," in Proc. Algorithms, Technol., Appl. for Multispectral Hyperspectral Imagery XXV, vol. 10986, 2019.
- [20] Y. C. Kim, H.-G. Yu, J.-H. Lee, D.-J. Park, and H.-W. Nam, "Hazardous gas detection for FTIR-based hyperspectral imaging system using DNN and CNN," in Proc. Electro-Opt. Infrared Syst.: Technol. Appl. XIV, vol. 10433, 2017.
- [21] L. Zhang, J. Wang, and Z. An, "Classification method of CO₂ hyperspectral remote sensing data based on neural network," Comput. Commun., vol. 156, pp. 124–130, 2020.

- [22] S. Kumar, C. Torres, O. Ulutan, A. Ayasse, D. Roberts, and B. S. Manjunath, "Deep remote sensing methods for methane detection in overhead hyperspectral imagery," in Proc. IEEE/CVF Winter Conf. Appl. Comput. Vis., 2020, pp. 1776–1785.
- [23] R. Gu, "Methane gas emission detection using deep learning and hyperspectral imagery," in Proc. IEEE 3rd Int. Conf. Front. Technol. Inf. Comput., 2021, pp. 36–44.
- [24] S. Henrot, J. Chanussot, and C. Jutten, "Dynamical spectral unmixing of multitemporal hyperspectral images," IEEE Trans. Image Process., vol. 25, no. 7, pp. 3219–3232, Jul. 2016.
- [25] Z. Shi, W. Tang, Z. Duren, and Z. Jiang, "Subspace matching pursuit for sparse unmixing of hyperspectral data," IEEE Trans. Geosci. Remote Sens., vol. 52, no. 6, pp. 3256–3274, Jun. 2014.
- [26] G. Tochon, D. Pauwels, M. D. Mura, and J. Chanussot, "Unmixing-based gas plume tracking in LWIR hyperspectral video sequences," in Proc. 8th Workshop Hyperspectral Image Signal Process.: Evol. Remote Sens., 2016, pp. 1–5.
- [27] N. Fiscante, P. Addabbo, F. Biondi, G. Giunta, and D. Orlando, "Unsupervised sparse unmixing of atmospheric trace gases from hyperspectral satellite data," IEEE Geosci. Remote Sens. Lett., vol. 19, 2022, Art. no. 6006405.
- [28] R. Harig and G. Matz, "Toxic cloud imaging by infrared spectrometry: A scanning FTIR system for identification and visualization," Field Anal. Chem. Technol., vol. 5, no. 1–2, pp. 75–90, 2001.
- [29] M. Planck, The Theory of Heat Radiation. Philadelphia, PA, USA: P. Blakiston's Son & Co., 1914.
- [30] Y. Gür, "Detection and identification of greenhouse gases using infrared hyperspectral imagery," M.Sc. Dissertation, Inf. Syst. Dept. Middle East Tech. Univ., Ankara, Turkey, 2017.